Curve Evolution with A Dual Shape Similarity and Its Application to Segmentation of Left Ventricle

Jonghye Woo[1], Byung-Woo Hong[2], Amit Ramesh[3], Guido Germano[3], C. -C. Jay Kuo[1] and Piotr Slomka[3]

[1]Department of Electrical Engineering, University of Southern California, Los Angeles, CA 90089-2564, USA
[2]School of Computer Science and Engineering, Chung-Ang University, Seoul, 156-756, Korea
[3]Departments of Imaging and Medicine, Cedars-Sinai Medical Center, Los Angeles, CA, USA

ABSTRACT

Automated image segmentation has been playing a critical role in medical image analysis. Recentl, Level Set methods have shown an efficacy and efficiency in various imaging modalities. In this paper, we present a novel segmentation approach to jointly delineate the boundaries of epi- and endocardium of the left ventricle on the Magnetic Resonance Imaging (MRI) images in a variational framework using level sets, which is in great demand as a clinical application in cardiology. One strategy to tackle segmentation under undesirable conditions such as subtle boundaries and occlusions is to exploit prior knowledge which is specific to the object to segment, in this case the knowledge about heart anatomy. While most left ventricle segmentation approaches incorporate a shape prior obtained by a training process from an ensemble of examples, we exploit a novel shape constraint using an implicit shape prior knowledge, which assumes shape similarity between epi- and endocardium allowing a variation under the Gaussian distribution. Our approach does not demand a training procedure which is usually subject to the training examples and is also laborious and time-consuming in generating the shape prior. Instead, we model a shape constraint by a statistical distance between the shape of epi- and endocardium employing signed distance functions. We applied this technique to cardiac MRI data with quantitative evaluations performed on 10 subjects. The experimental results show the robustness and effectiveness of our shape constraint within a Mumford-Shah segmentation model in the segmentation of left ventricle from cardiac MRI images in comparison with the manual segmentation results.

Keywords: Image Segmentation, Level Set, Dual shape constraint, Prior shape knowledge

1. INTRODUCTION

Cardiac MRI is widely recognized as the gold standard for volumetric analysis of the left ventricle (LV). Accurate segmentation of LV, particularly delineating the epi- and endocardium, is a fundamental and crucial prerequisite for the derivation of quantitative heart parameters such as wall thickening [1], end-diastolic volume (EDV), end-systolic volume (ESV), ejection fraction (EF), and myocardial mass [2].

Medical Imaging 2009: Image Processing, edited by Josien P. W. Pluim, Benoit M. Dawant,
Proc. of SPIE Vol. 7259, 72593T · © 2009 SPIE
CCC code: 1605-7422/09/$18 · doi: 10.1117/12.814142

In general, segmentation in medical images remains to be a challenging problem since not only should the unique imaging properties be captured but there also exist intrinsic problems associated with image quality such as low contrast, occlusions, image noise, and other complex phenomena which would make robust and accurate segmentation difficult. Several general image segmentation approaches have been proposed so far. One of the widely used segmentation methods is the edge-based segmentation method, which includes the use of edge operators and active contours called snakes [3, 4]. The snake technique evolves a curve defined in the image domain under the influence of internal and external forces. In classical active contour models, an edge detector is used to derive the external force. They detect objects with edges defined by gradients. This approach has several limitations.

First, the underlying image may suffer from low contrast and noise and the segmentation accuracy can be affected accordingly. Second, it is difficult to deal with topological change where curve parameterization is required. On the other hand, the region-based approach adopts a more global partitioning method that integrates intensity over the whole image domain [5, 6]. The region-based level set method represents curves implicitly as the zero level set of a scalar function. It can deal with topological change easily. Also, the region-based approach is more robust than the edge-based approach when the contrast between the object and the background is low.

Recently, the model-based approach [4, 7, 8] has gained a lot of attention as a solution to image segmentation problems with incomplete image information. It incorporates prior knowledge to improve the segmentation robustness and accuracy caused by poor image contrast, noise and missing boundaries. The prior shape model can be obtained using either explicit or implicit contour representations. The parametric point distribution model [9] with landmarks is an example of the explicit representation. However, the explicit boundary representation has several drawbacks such as fixed topology or pairwise correspondence.

To overcome these drawbacks, the level set method is employed for implicit representation. Segmentation with prior information was adopted in the level set method before [4, 7, 8]. The implicit contour representation has several advantages over the explicit one in that it does not depend on a specific parameterization or a shape dissimilarity measure. Thus, it can handle topological change more easily.

In either explicit or implicit contour representation, principal component analysis (PCA) has been widely used to get the shape prior. For example, Leventon *et al.* [10] proposed a shape prior model to restrict the flow of the geodesic active contour, where the prior was derived by performing PCA on a collection of signed distance function of the training shape. Most previous work [4, 11] tackled ill-posedness due to noise or subtle boundary by incorporating the explicit statistical shape prior. Given a set of training shapes, the prior information can be incorporated in the segmentation process. Although the shape-based method has led to successful segmentation results in [4, 11], they demand a manual segmented training data set, which is labor intensive.

It is worthwhile to point out that in cardiac MRI the detection of epicardium is more challenging than that of endocardium since the background contrast is lower than the blood pool contrast, resulting in a partially occluded epicardium boundary. Besides, it has a heterogeneous characteristics due to various structures immediately adjacent to the heart.

To address these limitations, we propose a segmentation algorithm by introducing a novel shape constraint and apply it to cardiac MRI segmentation of LV; namely, the implicit shape prior, without a training procedure based on the assumption that the endocardium and epicardium shapes are anatomically similar. Specifically, we formulate this problem as a region-based coupling level set segmentation [5, 12]. Cardiac MRI data are used in our experiment and quantitative tests of 10 subjects in end-diastolic (ED) and end-systolic (ES) phase demonstrate the accuracy and robustness of the proposed approach.

2. METHODS

2.1. Multi-phase Region-based Segmentation Scheme

We need to extract two structures, endocardium and epicardium, that are assumed to have similar shapes simultaneously in a single image. Note that one shape is located inside of the other. We propose a multi-phase segmentation scheme where the boundary of most probable structures of interest is jointly estimated. We model the boundaries of the epi- and endocardium as the zero level sets of two signed distance functions, $\phi_1(x)$ and $\phi_2(x)$, where $\{x|\phi_1(x)=0\}$ represents the endocardium boundary and $\{x|\phi_2(x)=0\}$ represents the epicardium boundary, respectively. The observed image I can be divided into three disjoint regions as:

$$\begin{cases} endocardium\,(blood\ pool) = \Omega_1 = \{x \in \Omega | \phi_1(x) > 0\}, \\ epicardium\,(myocardium) = \Omega_2 = \{x \in \Omega | \phi_1(x) < 0 \wedge \phi_2(x) > 0\}, \\ extracardiac\ structure = \Omega_b = \{x \in \Omega | \phi_2(x) < 0\} \end{cases}$$

Then we have an image model $I = c_1\chi_1 \wedge \chi_2 + c_2(1-\chi_1) \wedge \chi_2 + c_b(1-\chi_1) \wedge (1-\chi_2)$ where χ_1 and χ_2 are characteristic functions that specify the regions Ω_1 and Ω_2 respectively. Assuming this piecewise constant image model, the energy, called data fidelity term, that measures a discrepancy of intensities between given image and its ideal image model is defined by:

$$E_{data}(\phi_1, \phi_2) = \int_\Omega H(\phi_1(x))|I - c_1|^2 dx + \int_\Omega (1 - H(\phi_1(x)))H(\phi_2(x))|I - c_2|^2 dx$$
$$+ \int_\Omega (1 - H(\phi_1(x)))(1 - H(\phi_2(x)))|I - c_b|^2 dx$$

In the optimization, keeping ϕ_1 and ϕ_2 fixed, the average constant intensity, c_1, c_2 and c_b, can be updated as follows:

$$\begin{cases} c_1 = \dfrac{1}{|\Omega_1|}\int_\Omega IH(\phi_1)dx, \\ c_2 = \dfrac{1}{|\Omega_2|}\int_\Omega I(1-H(\phi_1))H(\phi_2)dx, \\ c_b = \dfrac{1}{|\Omega_b|}\int_\Omega I(1-H(\phi_2))dx \end{cases}$$

In addition to this model fitting, it is also preferable to obtain smooth segmentation results which leads to have the following regularization term:

$$E_{reg}(\phi_1,\phi_2) = \int_\Omega |\nabla H(\phi_1(x))|dx + \int_\Omega |\nabla H(\phi_2(x))|dx$$

In order to attract the segmenting curve toward the location of high contrast, we also introduce the following external energy using the edge indicator function:

$$E_{ext}(\phi_2) = \int_\Omega gH(-\phi_2)dx\,,$$

where $g = \dfrac{1}{1+|\nabla G_\sigma * I|^2}$ and G_σ is the Gaussian kernel with standard deviation σ.

When the function g is constant 1, the external energy functional is the area of the region $\Omega^-_{\phi_2} = \{x|\phi_2(x) < 0\}$.

Thus the external energy can be considered as the weighted area of $\Omega^-_{\phi_2}$

The segmentation model using the above three energy terms may fail to extract the structures of interest in the presence of missing or subtle boundaries. It is desired to incorporate prior knowledge on the objects of interest to deal with such difficulties and consequently we propose the following shape prior model that does not require explicit training data.

2.2. Shape constraint

The data fidelity term may be insufficient to extract the structures of interest in the presence of missing or subtle boundaries. Thus shape prior knowledge needs to be incorporated to deal with those obstacles and avoid local minima. Instead, we propose to use a shape constraint prior, implicit shape prior knowledge, between structures of interest without a need of training data.

The novel shape prior knowledge assumes that the shape of one object is similar to the shape of the other allowing variation in a statistical framework. We first define a shape distance between two regions of interest by $\phi_1(x)$ - $\phi_2(x)$ within the intersection of Ω_1 and Ω_2. Then, the shape distance $D(x)$ following the Gaussian distribution is given as:

$$p(D|\mu,\sigma) = \frac{1}{\sqrt{2\pi\sigma^2}} e^{-\frac{(\phi_2(x)-\phi_1(x)-\mu)^2}{2\sigma^2}} (1-H(\phi_1(x)))H(\phi_2(x)),$$

where the shape variation is subject to the choice of σ whose value is proportional to the allowable deformation between two shapes. Then, the shape constraint is defined as follows:

$$E_{shape}(\phi_1,\phi_2) = \log p(D|\mu,\sigma),$$

where μ is optimized from the closed form formula and σ can be chosen as constant empirically based on the deformation properties of the regions of interest to segment.

2.3. Energy minimization

The optimal solution to our problem should minimize the following energy:

$$E_{total}(\phi_1,\phi_2) = E_{data}(\phi_1,\phi_2) + \alpha E_{reg}(\phi_1,\phi_2) + \beta E_{shape}(\phi_1,\phi_2) + \lambda E_{ext}(\phi_1,\phi_2),$$

where α controls the smoothness of segmenting shapes, β weights the significance of the shape prior knowledge that specifies an allowable variation in distance between two shapes, and λ is a coefficient of the external energy which helps speed up the curve evolution.

A gradient descent approach is used as a minimization scheme and alternative minimization with respect to ϕ_1 and ϕ_2 is performed. We omit the detailed derivation of the associated Euler-Lagrange equations due to the space constraints.

For numerical implementation, we use the following approximations for the Heaviside function and the Dirac delta measure as defined in [5].

$$\delta(z) = \begin{cases} 0, \text{ if } |z| > \varepsilon \\ \frac{1}{2\varepsilon}\left[1+\cos(\frac{\pi z}{\varepsilon})\right], \text{ if } |z| \le \varepsilon \end{cases}$$

and

$$H(z)=\begin{cases}1, \text{if } z>-\varepsilon \\ 0, \text{if } z<-\varepsilon \\ \frac{1}{2}\left[1+\frac{z}{\varepsilon}+\frac{1}{\pi}\sin(\frac{\pi z}{\varepsilon})\right], \text{if } |z|\le\varepsilon\end{cases}$$

3. RESULTS

The proposed algorithm is implemented and tested on cardiac MRI at ED and ES phases of 10 subjects, followed by quantitative comparison to expert manual segmentation previously obtained. The images were acquired on a clinical 1.5T MRI scanner (Siemens Sonata, Erlangen, Germany). The imaging parameters were as follows: field of view = 350mm, matrix = 255 × 192 to 255 × 255, slice thickness = 8mm, slice gap = 2mm, TE/TR = 1.6/3.1 msec, pixel bandwidth = 930 kHz, flip angle = 60_ and segment size = 5-9 lines depending on heart rate. We used two circles from the endocardium center as manual initialization.

The mean values of EDV, ESV and LVEF calculated from 10 studies by using manual segmentation and proposed algorithm are presented in Table 1 and Bland-Altman plot is provided in Figure 3. Segmentation results of 2D and 3D volume for three cases are also presented in Figure 1.

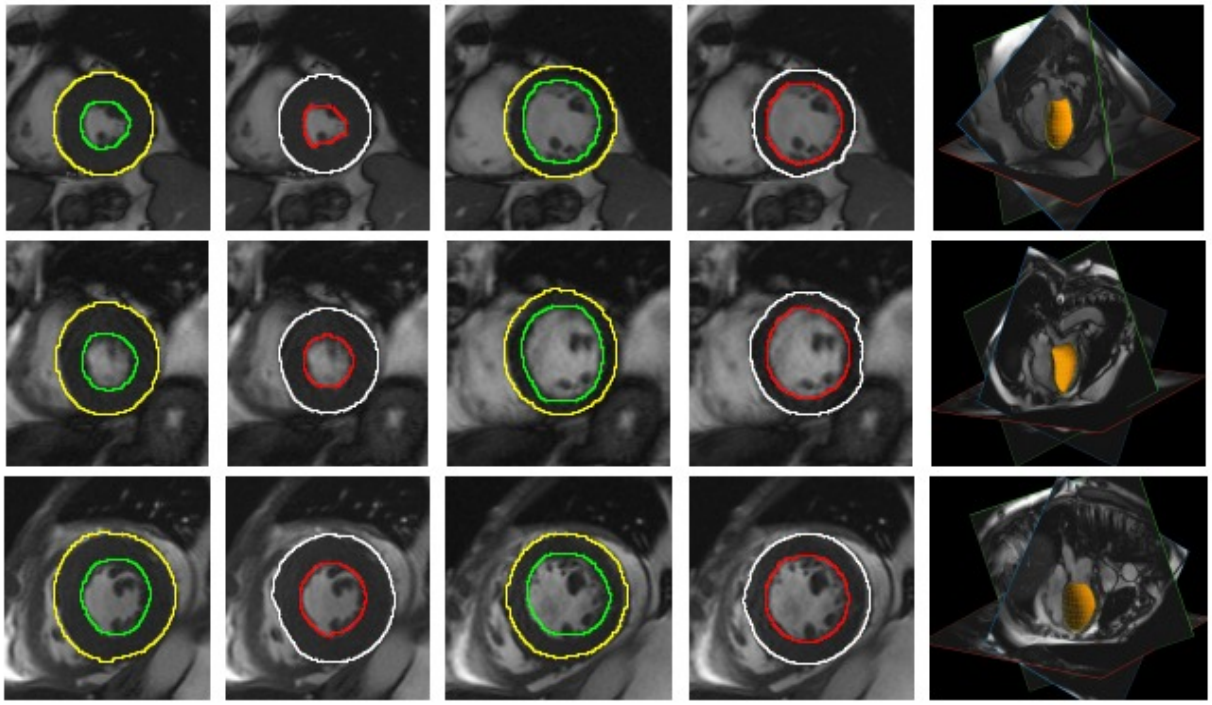

Fig. 1. Experimental results with ED and ES phases of three subjects (from top to bottom) shown on 2 selected slices in each case. Manual segmentation results of endocardium (green) and epicardium (yellow) are shown in first and third column and results of proposed algorithm are presented with endocardium (red) and epicardium (white) using same images in second and fourth column. Automatically segmented, 3D endocardial surface (orange) with epicardial surface (yellow mesh) is presented in the rightmost column. Algorithm parameters were selected empirically and were the same same for all images (α = 400, β = 30, λ =400 and σ = 2).

Table 1. Comparison of the manual segmentation and proposed algorithm

	Manual Segmentation	**Proposed Segmentation**
EDV (ml)	140 ± 44	139 ± 41
ESV (ml)	69 ± 45	68 ± 49
LVEF (%)	55 ± 16	55 ± 19

The mean values of EDV, ESV and LVEF calculated from 10 studies by using manual segmentation and proposed algorithm are presented in Table 1 and Bland-Altman plot is provided in Figure 2. Segmentation results of 2D and 3D volume for three cases are also presented in Figure 1.

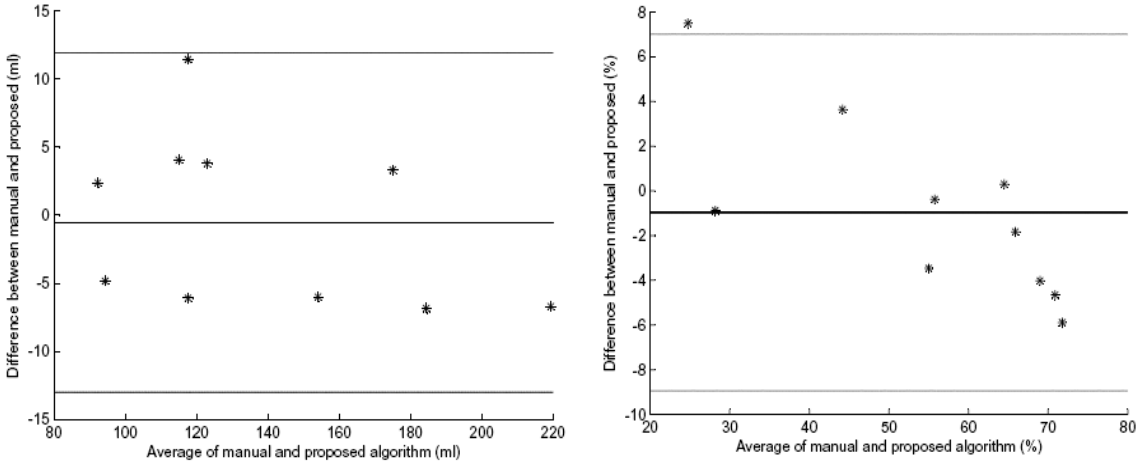

(a) EDV (b) LVEF

Fig. 2. Bland-Altman plots for EDV and LVEF

5. CONCLUSION

We have proposed a novel shape constraint to segment the epi- and endocardium of LV simultaneously. This shape constraint assumes the dual shape similarity between epi- and endocardium and its agreement with visual segmentation has been shown by the experimental results on cardiac MRI data. Currently, the only manual interaction is required at the initialization step that is desired to be specified automatically.

The segmentation algorithm incorporating our implicit shape prior knowledge can be used to segment related shapes simultaneously. It can be applied to segmentation of the epi- and endocardium of LV from cardiac MRI. We achieved robust results in initial evaluation.

REFERENCES

[1] Prasad, M., Ramesh, A., Kavanagh, P., Gerlach, J., Germano, G., Berman, D. S., and Slomka, P. J. "Myocardial wall thickening from gated Magnetic Resonance images using Laplace's equation." *SPIE Medical Imaging*. (2009)

[2] Frangi, A. F., Niessen, W. J., and Viergever, M. A. "Three-dimensional modeling for functional analysis of cardiac images: a review." *IEEE Trans Med Imaging*, 20(1), 2-25. (2001)

[3] Kass, M., Witkin, A., and Terzopoulos, D. "Snakes: Active contour models." *International Journal of Computer Vision*, 1(4), 321-331. (1998)

[4] Yezzi, A., Tsai, A., and Willsky, A. "A fully global approach to image segmentation via coupled curve evolution equations." *Journal of Visual Communication and Image Representation*, 13, 195-216. (2002)

[5] Chan, T. F., and Vese, L. A. "Active contours without edges." *IEEE Trans Image Processing*, 10(2), 266-277. (2001)

[6] Mumford, D., and Shah, J. "Optimal approximation by piecewise smooth functions and associated variational problems." *Commun. Pure Appl. Math*, 42, 577-685. (1989)

[7] Cremers, D., Osher, S. J., and Soatto, S. "Kernel density estimation and intrinsic alignment for shape priors in level set segmentation." *International Journal of Computer Vision*, 69(3), 335-351. (2006)

[8] Rousson, M., Paragios, N., and Deriche, R. "Implicit active shape models for 3d segmentation in mri imaging." *MICCAI*, 2217, 209-216. (2004)

[9] Cootes, T. F., Taylor, C. J., Cooper, D. H., and Graham, J. "Active shape models-their training and application." *Computer Vision and Image Understanding*, 61(1), 38-59. (1995)

[10] Leventon, M., Grimson, W., and Faugeras, O. "Statistical shape influence in geodesic active contours." *CVPR*, 316-323. (2000)

[11] Paragios, N. "A level set approach for shape-driven segmentation and tracking of the left ventricle." *IEEE Trans Med Imaging*, 22(6), 773-6. (2003)

[12] Vese, L. A., and Chan, T. F. " A Multiphase Level Set Framework for Image Segmentation Using the Mumford and Shah Model." *International Journal of Computer Vision*, 50(3), 271-293. (2002)